Robust Stabilization of Elastic Joint Robots by ESP and PID Control: Theory and Experiments

Keppler, Manuel; Raschel, Clara; Wandinger, David; Stemmer, Andreas; Ott, Christian

Robust Stabilization of Elastic Joint Robots by ESP and PID Control: Theory and Experiments

Manuel Keppler[1], and Clara Raschel[1], David Wandinger[1], Andreas Stemmer[1] and Christian Ott[1,2]

***Abstract*—This work addresses the problem of global set-point control of elastic joint robots by combining elastic structure preserving (ESP) control with non-collocated integral action. Despite the popularity and extensive research on PID control for rigid joint robots, such schemes largely evaded adoption to elastic joint robots. This is mainly due to the underactuation inherent to these systems, which impedes the direct implementation of PID schemes with non-collocated (link position) feedback. We remedy this issue by using the recently developed concept of "quasi-full actuation," to achieve a link-side PID control structure with "delayed" integral action. The design follows the structure preserving design philosophy of ESP control and ensures global asymptotic stability and local passivity of the closed loop. A key feature of the proposed controller is the switching logic for the integral action that enables the combination of excellent positioning accuracy in free motion with compliant manipulation in contact with the environment. Its performance is evaluated on an elastic joint testbed and a compliant robot arm. The results demonstrate that elastic robots may achieve positioning accuracy comparable to rigid joint robots.**

***Index Terms*—PID control, Elastic joint robot, Underactuation.**

I. Introduction

THE introduction of lightweight robot arms enabled compliant manipulation in contact with unknown environments and safe interaction with humans [1]–[3]. A major challenge inherent to the control design for such lightweight robots is the flexibility introduced into the robot joints, which is usually due to gear elasticity or the compliance of torque sensors. The control design became further challenging with the advent of robots with series elastic actuators (SEA) or variable impedance actuators [4]. In these articulated soft robots (ASRs), one deliberately incorporates highly compliant elements into the drive train with a stiffness that is low enough that these elements can be exploited as energy storage. All systems mentioned above are underactuated since the number of degrees of freedom is greater than the number of actuators. The implied loss of the matching property between control actions and outputs (non-collocation) impedes a direct implementation of PID-like controllers with link position feedback.

However, for such systems to be commercially attractive, combining safe and compliant behavior in contact with high positioning accuracy in free motion is paramount. The former has been subject to extensive research in the past and present years [2], [3], [5]–[9]. Additionally, several works [10]–[14] proposed robust controllers using integral action to address the latter. A review of the literature reveals that most of the experimental evaluations are concerned with robot arms, where parasitic effects cause the joint flexibility [10], [11], [14]; thus, the joint stiffness is usually relatively high, and the rigid body part gives a good approximation of the dominating dynamics. A lack of experimental analysis of integrator-based schemes on highly compliant robot arms exists, which raises the question of whether such systems, as shown in Fig. 1, can achieve a position accuracy comparable to that of rigid joint robots. This paper aims at to closing this gap.

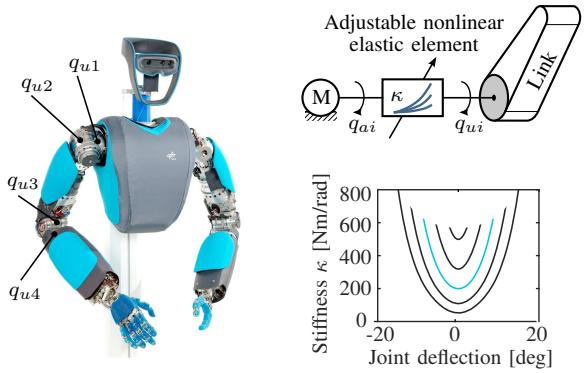

Figure 1. DLR *David*: A soft robot with variable stiffness actuators. [15]

Recently, we recently proposed the concept of elastic structure preserving (ESP) control for ASRs, which is based on the idea of preserving the structure of the open loop dynamics [16] but unlike [17], implements damping directly on the link side rather on the motor side, while also achieving motion tracking. In [8], we extended this approach to full Cartesian impedance control by achieving a link-side PD behavior.

The non-collocated PD feedback in [8] globally asymptotically stabilizes a desired set-point if the gravity force is balanced or compensated. Such an approach requires accurate knowledge of the gravitational forces. Using the best estimate usually results in (small) steady-state errors necessitating robust control. If a constant bounded disturbance occurs on a rigid joint robot, it is well known that adding an integral action to PD feedback can eliminate the resulting steady-state error [13], [18], [19]. Further, it allows for dealing with (non-perfectly compensated) gravity forces, which to some extent, can be considered a constant disturbance (from the local point of view) [20]. Motivated by this observation, we exploit the concept of quasi-full actuation [21] to extend the ESP controller [8] to a link-side PID control structure. Specifically, we adopt the

Manuscript received: February, 24, 2022; Accepted June, 8, 2022. This paper was recommended for publication by Editor Clement Gosselin upon evaluation of the Associate Editor and Reviewers' comments. DOI: see top of this page.

[1]First Author and Third Author are with the Institute of Robotics and Mechatronics, German Aerospace Center (DLR), 82234 Wessling, Germany mnl.kpplr@gmail.com

[2]The last author is with the Automation and Control Institute, TU Wien, 1040 Vienna, Austria.

Digital Object Identifier (DOI): see top of this page.

"delayed" linear PID controller proposed by Loria [18] and combine it with gravity compensation [22]. Our approach is motivated by the following observations.

Gravity in some manipulators, can range from zero up to 30 % or more of the maximum permissible torque [20]. For a PID controller with constant gains, this implies that transients in point-to-point control can exhibit substantial differences according to the type of motion required (going up or down) or the operational configurations [20]. The proposed controller achieves a uniform transient throughout the entire manipulator workspace by combing PID feedback with gravity compensation (up to the aforementioned model uncertainty). It is customary to activate the integral action only when the manipulator is near its desired configuration to avoid overshooting and to deactivate it when the error is too large [20]. The delayed PID controller [18] allows for a theoretical treatment of this heuristic idea. In summary, this work contributes:

- A "delayed" PID controller [18] for elastic joint robots, with non-collocated feedback, which ensures global asymptotic stabilization. By combining integral action with gravity [22] compensation, this works aims at improving positioning accuracy with minimal overshooting.
- A closed-loop that is locally passive with respect to external forces and a linear sum of link velocity and position errors in PID mode, and satisfying standard passivity in PD mode.
- A controller that combines high positioning accuracy in free motion with compliant manipulation in contact. Experimental evaluations demonstrate that an elastic manipulator may achieve positioning accuracy comparable to that of a rigid one.

This paper is organized as follows. Section II states the considered model, and Section III recalls some fundamentals for our main contribution. Section IV and V present locally stable PID controller for systems with linear and nonlinear elasticities, respectively. Our main result, a delayed PID controller, is presented in VI. Section VII introduces the experimental setup, Section VIII reports extensive experimental results, and Section IX concludes the paper.

Throughout and this paper, we denote by $\lambda_{\mathrm{m}}(\boldsymbol{A})$ and $\lambda_{\mathrm{M}}(\boldsymbol{A})$ the smallest and largest eigenvalues of a symmetric positive-definite bounded matrix $\boldsymbol{A}(\boldsymbol{x})$ for any $\boldsymbol{x} \in \mathbb{R}^n$.

II. Model

We consider an elastic joint robot satisfying Spong's model [23] with kinetic energy $\mathcal{T}(\boldsymbol{q}, \dot{\boldsymbol{q}}) = \frac{1}{2}\dot{\boldsymbol{q}}^{\mathrm{T}}\mathcal{M}(\boldsymbol{q}_u)\dot{\boldsymbol{q}}$, where $\boldsymbol{q}$ represents the n generalized coordinates, which can be partitioned into unactuated and actuated degrees of freedom $\boldsymbol{q}_u, \boldsymbol{q}_a \in \mathbb{R}^{n/2}$ such that $\boldsymbol{q} = (\boldsymbol{q}_u, \boldsymbol{q}_a)$. Matrix $\mathcal{M} = \mathcal{M}^{\mathrm{T}} = \operatorname{diag}(\boldsymbol{M}(\boldsymbol{q}_u), \boldsymbol{B}) \succ 0$ denotes the generalized inertia matrix, where $\boldsymbol{M}(\boldsymbol{q}_u)$ and $\boldsymbol{B}$ are the inertia matrices associated with the rigid robot dynamics and the reflected motor inertias. The gravitational, $\boldsymbol{g}(\boldsymbol{q}_u)$, and elastic forces are derived from the potential energies $\mathcal{V}_g(\boldsymbol{q}_u)$ and $\mathcal{V}_e(\boldsymbol{\varphi}) = \frac{1}{2}\boldsymbol{\varphi}^{\mathrm{T}}\boldsymbol{K}\boldsymbol{\varphi}$, $\boldsymbol{\varphi} = \boldsymbol{q}_a - \boldsymbol{q}_u$, where $\boldsymbol{K}$ is the diagonal matrix of the joint stiffness values. Let $\mathcal{Q}' \in \mathbb{R}^n$ represent the generalized external forces, with forces acting on the unactuated and actuated subsystems partitioned so that $\mathcal{Q}' = (\mathcal{Q}'_u, \mathcal{Q}'_a)$. Then, the associated Euler–Lagrange equations are

$$\begin{aligned} \boldsymbol{M}(\boldsymbol{q}_u)\ddot{\boldsymbol{q}}_u + \boldsymbol{C}(\boldsymbol{q}_u, \dot{\boldsymbol{q}}_u)\dot{\boldsymbol{q}}_u + \boldsymbol{g}(\boldsymbol{q}_u) - \boldsymbol{K}\boldsymbol{\varphi} &= \mathcal{Q}'_u, \\ \boldsymbol{B}\ddot{\boldsymbol{q}}_a + \boldsymbol{K}\boldsymbol{\varphi} &= \boldsymbol{u} + \mathcal{Q}'_a, \end{aligned} \tag{1}$$

where $\boldsymbol{C}(\boldsymbol{q}_u, \dot{\boldsymbol{q}}_u)$ is the Coriolis and centrifugal matrix connected with the rigid body dynamics, and $\boldsymbol{u}$ is the generalized input force exerted by the $n/2$ actuators. Introducing

$$\mathcal{K}_e = \begin{bmatrix} \boldsymbol{K} & -\boldsymbol{K} \\ -\boldsymbol{K} & \boldsymbol{K} \end{bmatrix}, \tag{2}$$

allows writing the elastic potential energy compactly as $\mathcal{V}_e = \frac{1}{2}\boldsymbol{q}^{\mathrm{T}}\mathcal{K}_e\boldsymbol{q}$. For notational simplicity, we shall refrain from writing the explicit dependency on $\boldsymbol{q}, \dot{\boldsymbol{q}}$ of any coefficient. In this work, we assume the following:

Assumption 1. *For all $\boldsymbol{q}_u \in \mathbb{R}^{n/2}$, the matrix $\mathcal{M}$ is positive definite, and there exist some positive constants d_m and d_M such that $d_m\boldsymbol{I} < \mathcal{M} < d_M\boldsymbol{I}$.*[1]

Property 1. *For a suitable choice of $\boldsymbol{C}$ in* (1)*, we have that $\dot{\mathcal{M}} = \mathcal{C} + \mathcal{C}^T$ [25], where $\mathcal{C} = \operatorname{diag}(\boldsymbol{C}, \boldsymbol{0})$. Moreover, the matrix $\boldsymbol{C}(\boldsymbol{x}, \boldsymbol{y})$ is bounded in $\boldsymbol{x}$ and linear in $\boldsymbol{y}$ such that $\|\boldsymbol{C}(\boldsymbol{x}, \boldsymbol{y})\| \leq k_C\|\boldsymbol{x}\|\,\|\boldsymbol{y}\|$ [24].*

III. Problem Formulation and Preliminary Results

We consider the link positions $\boldsymbol{q}_u$ as outputs with constant desired values $\boldsymbol{q}_u^* \in \mathbb{R}^{n/2}$. The associated equilibrium motor positions, $\boldsymbol{q}_a^*$, are dictated by the equilibrium condition of (1), and for $\mathcal{Q}' = \boldsymbol{0}$, we get $\boldsymbol{q}_a^* = \boldsymbol{q}_u^* + \boldsymbol{K}^{-1}\boldsymbol{g}(\boldsymbol{q}_u^*)$. The output $\boldsymbol{q}_u$ is *non-collocated* with the input $\boldsymbol{u}$, which impedes direct the implementation of PID output-feedback control. We can remedy this issue by employing the concept of quasi-full actuation [21]. That is, we introduce the virtual motor coordinates $\bar{\boldsymbol{q}}_a$ and inputs $\bar{\boldsymbol{u}} = (\bar{\boldsymbol{u}}_u, \bar{\boldsymbol{u}}_a)$ and apply the coordinate and input transformation

$$\boldsymbol{q}_a = \bar{\boldsymbol{q}}_a + \boldsymbol{K}^{-1}\bar{\boldsymbol{u}}_u, \tag{3}$$

$$\boldsymbol{u} = \boldsymbol{B}\boldsymbol{K}^{-1}\ddot{\bar{\boldsymbol{u}}}_u + \bar{\boldsymbol{u}}_u + \bar{\boldsymbol{u}}_a, \tag{4}$$

as reported in [21] to (1) and obtain

$$\begin{aligned} \bar{\Sigma}_u\colon\ & \boldsymbol{M}\ddot{\boldsymbol{q}}_u + \boldsymbol{C}\dot{\boldsymbol{q}}_u + \boldsymbol{g}(\boldsymbol{q}_u) - \boldsymbol{K}(\bar{\boldsymbol{q}}_a - \boldsymbol{q}_u) = \bar{\boldsymbol{u}}_u + \mathcal{Q}'_u, \\ \bar{\Sigma}_a\colon\ & \boldsymbol{B}\ddot{\bar{\boldsymbol{q}}}_a + \boldsymbol{K}(\bar{\boldsymbol{q}}_a - \boldsymbol{q}_u) = \bar{\boldsymbol{u}}_a + \mathcal{Q}'_a, \end{aligned} \tag{5}$$

with the generalized coordinates $\bar{\boldsymbol{q}} = (\boldsymbol{q}_u, \bar{\boldsymbol{q}}_a)$. In this text, we shall exploit $\bar{\boldsymbol{u}}_u$ for implementing non-collocated PID feedback.

Remark 1. *If $\bar{\boldsymbol{u}}_u$ feeds back only the unactuated states, and possibly contains the time explicitly, then the coordinate transformation* (3) *establishes a one-to-one correspondence between the solutions $\boldsymbol{q}(t)$ and $\bar{\boldsymbol{q}}(t)$ of* (1) *and* (5)*, respectively. Thus, instead of studying and controlling the behavior of* (1)*, one can equivalently study and control the behavior of* (5)*.*

In summary, we are interested in designing a control law (dynamic state feedback) $\boldsymbol{u} = \boldsymbol{u}(\boldsymbol{q}, \dot{\boldsymbol{q}}, \boldsymbol{v})$, $\dot{\boldsymbol{v}} = \boldsymbol{f}(\boldsymbol{q}, \boldsymbol{v})$, such that the closed loop (1) with $\boldsymbol{u}$ is globally asymptotically stable at any setpoint $(\boldsymbol{q}, \dot{\boldsymbol{q}}, \boldsymbol{v}) = (\boldsymbol{q}^*, \boldsymbol{0}, \boldsymbol{0})$. In particular, we are interested in using the transformed dynamics (5) to implement a delay PID controller that achieves this objective.

[1] This is always the case for manipulators with only revolute joints. [24]

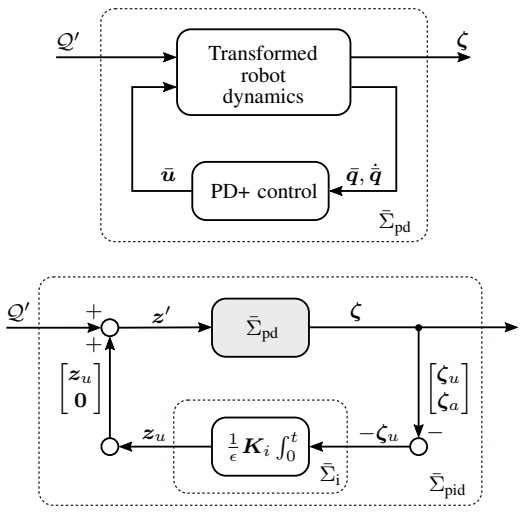

Figure 2. (**top**) Passivity of $\bar{\Sigma}_{pd}$ with respect to the output $\dot{\boldsymbol{q}}$ or $(\dot{\boldsymbol{q}} + \epsilon\tilde{\boldsymbol{q}})$ [27], where $\bar{\Sigma}_{pd}$ is the transformed robot dynamics (5) under PD plus gravity compensation control (7). (**bottom**) Feedback interconnection of the passive robot dynamics (under PD+ control) with a linear PI controller.

IV. PID Control for Linear Elasticities

Using the virtual input $\bar{\boldsymbol{u}}$, we can easily achieve local asymptotic stabilization of (5) with PID control. Since we aim at compensating for output steady-state errors, the following controller only feeds the link position error into the integrator. We extend the results of [26] to elastic joint robots.

Remark 2. *It is convenient to introduce the following definitions. Let $\boldsymbol{K}_{pu}, \boldsymbol{K}_i \in \mathbb{R}^{n/2}$ and $\mathcal{K}_v \in \mathbb{R}^n$ be symmetric positive definite matrices, $\mathcal{K}_p = \operatorname{diag}(\boldsymbol{K}_{pu}, \boldsymbol{0})$, and*

$$\begin{aligned} \tilde{\boldsymbol{q}} &= (\tilde{\boldsymbol{q}}_u, \tilde{\boldsymbol{q}}_a) = (\boldsymbol{q}_u - \boldsymbol{q}_u^*, \bar{\boldsymbol{q}}_a - \boldsymbol{q}_u^*), \\ \boldsymbol{v} &= (\boldsymbol{v}_u, \boldsymbol{0}) \in \mathbb{R}^n, \\ \boldsymbol{z} &= (\boldsymbol{z}_u, \boldsymbol{0}),\ \boldsymbol{z}' = \boldsymbol{z} + \mathcal{Q}' \in \mathbb{R}^n, \\ \boldsymbol{\zeta} &= (\boldsymbol{\zeta}_u, \boldsymbol{\zeta}_a) \in \mathbb{R}^n. \end{aligned} \tag{6}$$

Proposition 1. *Consider the transformed system* (5) *in closed loop with the PID control law*

$$\bar{\boldsymbol{u}} = -\mathcal{K}_p\tilde{\boldsymbol{q}} - \mathcal{K}_v\dot{\tilde{\boldsymbol{q}}} + \frac{\partial \mathcal{V}_g}{\partial \bar{\boldsymbol{q}}} + \boldsymbol{v}, \tag{7}$$

$$\dot{\boldsymbol{v}}_u = -\boldsymbol{K}_i\tilde{\boldsymbol{q}}_u, \quad \boldsymbol{v}_u(\boldsymbol{0}) = \boldsymbol{v}_{u0} \in \mathbb{R}^{n/2}, \tag{8}$$

with the definitions in Remark 2. Consider the signals

$$\boldsymbol{\zeta} = \epsilon\tilde{\boldsymbol{q}} + \dot{\tilde{\boldsymbol{q}}}, \quad \boldsymbol{z}_u = \boldsymbol{v}_u - \tfrac{1}{\epsilon}\boldsymbol{K}_i\tilde{\boldsymbol{q}}_u, \tag{9}$$

with $\boldsymbol{K}_{pu} - \frac{1}{\epsilon}\boldsymbol{K}_i > 0$, then there exists some constant $\epsilon > 0$ such that the resulting closed loop can be represented as the feedback interconnection of $\bar{\Sigma}_{pd}$ and $\bar{\Sigma}_I$, as in Fig. 2, with:

- *$\bar{\Sigma}_{pd}$ defines a locally OSP[2] mapping $\boldsymbol{z} + \mathcal{Q}' \mapsto \boldsymbol{\zeta}$.*
- *$\bar{\Sigma}_i$ defines an OSP mapping $-\boldsymbol{\zeta}_u \mapsto \boldsymbol{z}_u$.*

The closed loop is locally asymptotically stable at the origin $\boldsymbol{x} \triangleq (\tilde{\boldsymbol{q}}, \dot{\tilde{\boldsymbol{q}}}, \boldsymbol{z}_u) = \boldsymbol{0}$ for $\mathcal{Q}' = \boldsymbol{0}$.

[2]OSP: output strictly passive.

Proof of Proposition 1. It is convenient to introduce

$$\begin{aligned} \mathcal{K}_p &= \mathcal{K}_p' + \tfrac{1}{\epsilon}\operatorname{diag}(\boldsymbol{K}_i, \boldsymbol{0}), \\ \mathcal{K}' &= \mathcal{K}_p' + \mathcal{K}_e, \end{aligned} \tag{10}$$

where $\epsilon > 0$ is a (small) constant to be determined. First, we observe that $\bar{\boldsymbol{q}}_a - \boldsymbol{q}_u = \tilde{\boldsymbol{q}}_a - \tilde{\boldsymbol{q}}_u$ which implies that $\mathcal{K}_e\bar{\boldsymbol{q}} = \mathcal{K}_e\tilde{\boldsymbol{q}}$, such that making the substitution (7) and (5) gives

$$\mathcal{M}\ddot{\tilde{\boldsymbol{q}}} + \big(\mathcal{C} + \mathcal{K}_v\big)\dot{\tilde{\boldsymbol{q}}} + (\mathcal{K}_e + \mathcal{K}_p)\tilde{\boldsymbol{q}} = \boldsymbol{v} + \mathcal{Q}'. \tag{11}$$

Then, considering (9) and (10), we can write the error dynamics (5), (7) and (8) as (see also Fig. 2)

$$\bar{\Sigma}_{\text{pd}}\colon \mathcal{M}\ddot{\tilde{\boldsymbol{q}}} + (\mathcal{C} + \mathcal{K}_v)\dot{\tilde{\boldsymbol{q}}} + \mathcal{K}'\tilde{\boldsymbol{q}} = \boldsymbol{z} + \mathcal{Q}', \tag{12}$$

$$\bar{\Sigma}_{\text{i}}\colon \dot{\boldsymbol{z}}_u = -\boldsymbol{K}_i(\tilde{\boldsymbol{q}}_u + \tfrac{1}{\epsilon}\dot{\boldsymbol{q}}_u). \tag{13}$$

To show the postulated stability and passivity properties of the closed loop, we consider the following Lyapunov function candidate, which shall also serve as storage function:[3]

$$V(\boldsymbol{x}) = \mathcal{H}_{\text{pd}} + \mathcal{H}_{\text{i}}, \tag{14}$$

$$\mathcal{H}_{\text{i}}(\boldsymbol{z}_u) = \tfrac{1}{2}\epsilon\boldsymbol{z}_u^{\mathrm{T}}\boldsymbol{K}_i^{-1}\boldsymbol{z}_u, \tag{15}$$

$$\mathcal{H}_{\text{pd}}(\tilde{\boldsymbol{q}}, \dot{\tilde{\boldsymbol{q}}}) = \tfrac{1}{2}\big(\dot{\tilde{\boldsymbol{q}}}^{\mathrm{T}}\mathcal{M}\dot{\tilde{\boldsymbol{q}}} + \tilde{\boldsymbol{q}}^{\mathrm{T}}\mathcal{K}'\tilde{\boldsymbol{q}}\big) + \epsilon\tilde{\boldsymbol{q}}^{\mathrm{T}}\mathcal{M}\dot{\tilde{\boldsymbol{q}}}, \tag{16}$$

where ϵ is a sufficiently small constant satisfying:

$$\sqrt{\lambda_{\text{m}}(\mathcal{K}')/\lambda_{\text{M}}(\mathcal{M})} \geq \epsilon > 0, \tag{17}$$

$$2\lambda_{\text{m}}(\mathcal{K}')/\lambda_{\text{M}}(\mathcal{K}_v) \geq \epsilon > 0, \tag{18}$$

$$\tfrac{1}{2}\lambda_{\text{m}}(\mathcal{K}_v)/\big[(k_C\|\tilde{\boldsymbol{q}}\| + \lambda_{\text{M}}(\mathcal{M})\big] \geq \epsilon > 0, \tag{19}$$

where the existence of a constant $k_C > 0$ is ensured by Property 1. Condition (17) ensures that $\mathcal{H}_{\text{pd}}$ is a positive definite function; see Appendix X for details. Positive definiteness of V follows trivially. After some simplifications and using Property 1, we get for the time derivative of $\mathcal{H}_{\text{pd}}$ along the solutions of the closed-loop dynamics (12)

$$\begin{aligned} \dot{\mathcal{H}}_{\text{pd}} &= \dot{\tilde{\boldsymbol{q}}}^{\mathrm{T}}\boldsymbol{z}' - \dot{\tilde{\boldsymbol{q}}}^{\mathrm{T}}\mathcal{K}_v\dot{\tilde{\boldsymbol{q}}} + \epsilon\big(\dot{\tilde{\boldsymbol{q}}}^{\mathrm{T}}\mathcal{M}\dot{\tilde{\boldsymbol{q}}} + \tilde{\boldsymbol{q}}^{\mathrm{T}}\dot{\mathcal{M}}\dot{\tilde{\boldsymbol{q}}} + \tilde{\boldsymbol{q}}^{\mathrm{T}}\mathcal{M}\ddot{\tilde{\boldsymbol{q}}}\big), \\ &= \boldsymbol{\zeta}^{\mathrm{T}}\boldsymbol{z}' - \dot{\tilde{\boldsymbol{q}}}^{\mathrm{T}}\mathcal{K}_v\dot{\tilde{\boldsymbol{q}}} + \epsilon\big(\dot{\tilde{\boldsymbol{q}}}^{\mathrm{T}}\mathcal{M}\dot{\tilde{\boldsymbol{q}}} + \tilde{\boldsymbol{q}}^{\mathrm{T}}\big[\mathcal{C}^{\mathrm{T}}\dot{\tilde{\boldsymbol{q}}} - \mathcal{K}_v\dot{\tilde{\boldsymbol{q}}} - \mathcal{K}'\tilde{\boldsymbol{q}}\big]\big). \end{aligned} \tag{20}$$

Let us establish upper bounds on the following terms

$$\epsilon\dot{\tilde{\boldsymbol{q}}}^{\mathrm{T}}\mathcal{M}\dot{\tilde{\boldsymbol{q}}} \leq \epsilon\lambda_{\text{M}}(\mathcal{M})\|\dot{\tilde{\boldsymbol{q}}}\|^2, \tag{21}$$

$$\epsilon\dot{\tilde{\boldsymbol{q}}}^{\mathrm{T}}\mathcal{C}\tilde{\boldsymbol{q}} \leq \epsilon k_C\|\tilde{\boldsymbol{q}}\|\,\|\dot{\tilde{\boldsymbol{q}}}\|^2, \tag{22}$$

$$-\dot{\tilde{\boldsymbol{q}}}^{\mathrm{T}}\mathcal{K}_v\dot{\tilde{\boldsymbol{q}}} \leq -\tfrac{1}{2}\big(\dot{\tilde{\boldsymbol{q}}}^{\mathrm{T}}\mathcal{K}_v\dot{\tilde{\boldsymbol{q}}} + \lambda_{\text{m}}(\mathcal{K}_v)\|\dot{\tilde{\boldsymbol{q}}}\|^2\big), \tag{23}$$

$$-\epsilon\tilde{\boldsymbol{q}}^{\mathrm{T}}\mathcal{K}_v\dot{\tilde{\boldsymbol{q}}} \leq \epsilon\lambda_{\text{M}}(\mathcal{K}_v)\|\tilde{\boldsymbol{q}}\|\,\|\dot{\tilde{\boldsymbol{q}}}\|. \tag{24}$$

The inequalities (21) and (22) follow immediately from Property 1 and the results in [24, p. 256]. Knowing that $\mathcal{K}_v$ is positive definite, we get for the spectral norm $\|\mathcal{K}_v\| = \sqrt{\lambda_{\text{M}}(\mathcal{K}_v^{\mathrm{T}}\mathcal{K}_v)} = \lambda_{\text{M}}(\mathcal{K}_v)$, which implies (24). Next, from (20)–(24), we conclude that

$$\begin{aligned} \dot{\mathcal{H}}_{\text{pd}} &\leq -\epsilon\begin{bmatrix}\|\tilde{\boldsymbol{q}}\| \\ \|\dot{\tilde{\boldsymbol{q}}}\|\end{bmatrix}^{\mathrm{T}}\boldsymbol{Q}\begin{bmatrix}\|\tilde{\boldsymbol{q}}\| \\ \|\dot{\tilde{\boldsymbol{q}}}\|\end{bmatrix} + \delta + \boldsymbol{\zeta}^{\mathrm{T}}\boldsymbol{z}'; \\ \delta &= -\big\{\tfrac{1}{2}\lambda_{\text{m}}(\mathcal{K}_v) - \epsilon\big[k_C\|\tilde{\boldsymbol{q}}\| + \lambda_{\text{M}}(\mathcal{M})\big]\big\}\|\dot{\tilde{\boldsymbol{q}}}\|^2; \\ \boldsymbol{Q} &= \begin{bmatrix}\lambda_{\text{m}}(\mathcal{K}') & -\frac{1}{2}\lambda_{\text{M}}(\mathcal{K}_v) \\ -\frac{1}{2}\lambda_{\text{M}}(\mathcal{K}_v) & \frac{1}{2\epsilon}\lambda_{\text{m}}(\mathcal{K}_v)\end{bmatrix}. \end{aligned} \tag{25}$$

[3]Note that we can always substitute $\boldsymbol{q}_u = \tilde{\boldsymbol{q}}_u + \boldsymbol{q}_u^*$ to write storage and Lyapunov functions in terms of only the error coordinates.

Inequality (18) implies that $\boldsymbol{Q}$ is positive definite and (19) that $\delta \leq 0$. As the existence of $\delta \leq 0$ is connected to (19), we can conclude only local OSP for $\bar{\Sigma}_{pd}$. Next, let us establish passivity for the subsystem $\bar{\Sigma}_{\mathrm{i}}$ with the storage function $\mathcal{H}_{\mathrm{i}}$ in (15). Its time derivative along the solutions of $\bar{\Sigma}_{\mathrm{i}}$ is

$$\dot{\mathcal{H}}_{\mathrm{i}} = -\boldsymbol{z}_u^{\mathrm{T}} \boldsymbol{\zeta}_u. \tag{26}$$

We established the passivity properties of $\bar{\Sigma}_{\mathrm{pid}}$ and $\bar{\Sigma}_{\mathrm{i}}$.

Let $\mathcal{Q}' = \mathbf{0}$. Consider the set

$$B_\alpha = \{\boldsymbol{x} \in \mathbb{R}^{3n} \colon V(\boldsymbol{x}) \leq \alpha\}, \tag{27}$$

where α is the largest positive constant such that (19) holds, and thus $\dot{V}(\boldsymbol{x}) \leq 0$ for all $\boldsymbol{x} \in B_\alpha$. Knowing that V is positive definite and radially unbounded, and that $\dot{V} \leq 0$ for all $\boldsymbol{x} \in B_\alpha$, we conclude that the set is positively invariant (in words, if $\boldsymbol{x}(0) \in B_\alpha$ then $\boldsymbol{x}(t) \in B_\alpha$ for all $t \geq 0$) and qualifies as a domain of attraction for $\boldsymbol{x}(t)$. Local asymptotic stability of the origin $\boldsymbol{x} = \mathbf{0}$ can be shown by invoking Krasovskii–La'Salle's invariance principle [28, p. 129]. □

V. PID Control for Nonlinear Elasticities

In this section, we sketch an extension of Proposition 1 to a robot arm modeled by[4]

$$\begin{aligned} \boldsymbol{M}\ddot{\boldsymbol{q}}_u + \boldsymbol{C}\dot{\boldsymbol{q}}_u + \boldsymbol{g}(\boldsymbol{q}_u) - \boldsymbol{\psi}(\boldsymbol{q}_a - \boldsymbol{q}_u) &= \mathcal{Q}'_u, \\ \boldsymbol{B}\ddot{\boldsymbol{q}}_a + \boldsymbol{\psi}(\boldsymbol{q}_a - \boldsymbol{q}_u) &= \boldsymbol{u}, \end{aligned} \tag{28}$$

where the generalized elastic forces $\boldsymbol{\psi}$ satisfy:

Assumption 2. *The $\mathcal{C}^k$, $k \geq 3$, positive definite elastic potential $\mathcal{V}_e \colon \mathbb{R}^n \to \mathbb{R}$ is associated with the joint deflections $\boldsymbol{\varphi}$ such that the ith generalized elastic force $\psi_i(\varphi_i) = \partial \mathcal{V}_e(\boldsymbol{\varphi})/\partial \varphi_i$ and local stiffness $\kappa_i(\varphi_i) = \partial^2 \mathcal{V}_e(\boldsymbol{\varphi})/\partial \varphi_i^2$ satisfy:*

$$c_M \geq \sup_{\varphi \in \mathbb{R}^{n/2}} \|\kappa_i(\varphi_i)\| \geq c_m \quad \forall \varphi_i \in \mathbb{R}, \tag{29}$$

$$\varphi_i \psi_i(\varphi_i) \geq \beta \|\varphi_i\|^2 \quad \forall \varphi_i \in \mathbb{R}, \tag{30}$$

for some $c_m, c_M, \beta > 0$, and $\psi_i(0) = 0$.

Then, we can apply the coordinate and input transformation from [21]; that is, we apply the transformation

$$\boldsymbol{\psi}(\boldsymbol{\varphi}) = \boldsymbol{\psi}(\bar{\boldsymbol{\varphi}}) + \bar{\boldsymbol{u}}_u, \tag{31}$$

where $\bar{\boldsymbol{\varphi}} = \bar{\boldsymbol{q}}_a - \boldsymbol{q}_u = \tilde{\boldsymbol{q}}_a - \tilde{\boldsymbol{q}}_u$, and the intermediary input

$$\boldsymbol{u} = \boldsymbol{B}(\dot{\boldsymbol{A}} + \dot{\boldsymbol{a}}) + \bar{\boldsymbol{u}}_u + \boldsymbol{A}\bar{\boldsymbol{u}}_a + (\boldsymbol{I} - \boldsymbol{A})\boldsymbol{\psi}(\bar{\boldsymbol{\varphi}}), \tag{32}$$

to (1) which gives[5]

$$\begin{aligned} \boldsymbol{M}\ddot{\boldsymbol{q}}_u + \boldsymbol{C}\dot{\boldsymbol{q}}_u + \boldsymbol{g}(\boldsymbol{q}_u) - \boldsymbol{\psi}(\bar{\boldsymbol{q}}_a - \boldsymbol{q}_u) &= \bar{\boldsymbol{u}}_u + \mathcal{Q}'_u, \\ \boldsymbol{B}\ddot{\boldsymbol{q}}_a + \boldsymbol{\psi}(\bar{\boldsymbol{q}}_a - \boldsymbol{q}_u) &= \bar{\boldsymbol{u}}_a. \end{aligned} \tag{33}$$

Comparing (33) with (5), it is evident that we are now in a position to proceed analogously to the linear spring case. Applying the PID controller (7) to (33) yields the error dynamics

$$\bar{\Sigma}_{\mathrm{pd}} \colon \mathcal{M}\ddot{\tilde{\boldsymbol{q}}} + \big(\mathcal{C} + \mathcal{K}_v\big)\dot{\tilde{\boldsymbol{q}}} + \frac{\partial \mathcal{V}_e}{\partial \bar{\boldsymbol{q}}} + \mathcal{K}'_p \tilde{\boldsymbol{q}} = \boldsymbol{z} + \mathcal{Q}' \tag{34}$$

$$\bar{\Sigma}_{\mathrm{i}} \colon \dot{\boldsymbol{z}}_u = -\boldsymbol{K}_i(\tilde{\boldsymbol{q}}_u + \tfrac{1}{\epsilon}\dot{\boldsymbol{q}}_u) \tag{35}$$

Proposition 2. *The conclusion of Proposition 1 remains valid if the PID control law* (7)–(8) *is applied to the transformed system* (33)*, which results in the closed loop* (34)–(35)*.*

Sketch of Proof of Proposition 2. In the following, we sketch a proof by highlighting the modifications required compared to the proof of Proposition 1. Observing that the error dynamics (11) and (34) only differ in the potential forces suggests modifying the storage function (16) to

$$\mathcal{H}_{\mathrm{pd}}(\tilde{\boldsymbol{q}}, \dot{\tilde{\boldsymbol{q}}}) = \tfrac{1}{2}\big(\dot{\tilde{\boldsymbol{q}}}^{\mathrm{T}} \mathcal{M} \dot{\tilde{\boldsymbol{q}}} + \tilde{\boldsymbol{q}}^{\mathrm{T}} \mathcal{K}'_p \tilde{\boldsymbol{q}}\big) + \mathcal{V}_e(\bar{\boldsymbol{\varphi}}) + \epsilon \tilde{\boldsymbol{q}}^{\mathrm{T}} \mathcal{M} \dot{\tilde{\boldsymbol{q}}}. \tag{36}$$

Considering Assumption 2 and proceeding analogously to Appendix X, we conclude that $\mathcal{H}_{\mathrm{pd}}$ is a positive definite function. Considering that $\tilde{\boldsymbol{q}}^{\mathrm{T}}(\partial \mathcal{V}_e/\partial \bar{\boldsymbol{\varphi}}) = \bar{\boldsymbol{\varphi}}^{\mathrm{T}} \boldsymbol{\psi}(\bar{\boldsymbol{\varphi}})$, we get

$$\begin{aligned} \dot{\mathcal{H}}_{\mathrm{pd}} =& \boldsymbol{\zeta}^{\mathrm{T}} \boldsymbol{z}' - \dot{\tilde{\boldsymbol{q}}}^{\mathrm{T}} \mathcal{K}_v \dot{\tilde{\boldsymbol{q}}} + \\ & \epsilon\Big(\dot{\tilde{\boldsymbol{q}}}^{\mathrm{T}} \mathcal{M} \dot{\tilde{\boldsymbol{q}}} + \tilde{\boldsymbol{q}}^{\mathrm{T}} \Big[\mathcal{C}^{\mathrm{T}} \dot{\tilde{\boldsymbol{q}}} - \mathcal{K}_v \dot{\tilde{\boldsymbol{q}}} - \frac{\partial \mathcal{V}_e}{\partial \bar{\boldsymbol{q}}} - \mathcal{K}'_p \tilde{\boldsymbol{q}}\Big]\Big). \end{aligned} \tag{37}$$

with $\boldsymbol{z}'$ as in (6), and a positive lower bound on the terms:

$$\begin{aligned} &\tilde{\boldsymbol{q}}^{\mathrm{T}} \left[\frac{\partial \mathcal{V}_e}{\partial \bar{\boldsymbol{q}}} + \mathcal{K}'_p \tilde{\boldsymbol{q}}\right] \geq \beta \|\bar{\boldsymbol{\varphi}}\|^2 + \lambda_{\mathrm{m}}(\boldsymbol{K}_{pu} - \tfrac{1}{\epsilon}\boldsymbol{K}_i)\|\tilde{\boldsymbol{q}}_u\|^2 = \\ &\tilde{\boldsymbol{q}}^{\mathrm{T}} \underbrace{\begin{bmatrix} (\beta + \lambda_{\mathrm{m}}(\boldsymbol{K}_{pu} - \frac{1}{\epsilon}\boldsymbol{K}_i))\boldsymbol{I} & -\beta \boldsymbol{I} \\ -\beta \boldsymbol{I} & \beta \boldsymbol{I} \end{bmatrix}}_{\mathcal{K}_\beta} \tilde{\boldsymbol{q}} \geq \lambda_{\mathrm{m}}(\mathcal{K}_\beta)\|\tilde{\boldsymbol{q}}\|^2, \end{aligned}$$

where $\lambda_{\mathrm{m}}(\mathcal{K}_\beta) > 0$ follows from of $\boldsymbol{K}_{pu} - \frac{1}{\epsilon}\boldsymbol{K}_i > 0$ and $\beta > 0$. Using (17)–(19), (21)–(24) and the inequalities above:

$$\begin{aligned} \dot{\mathcal{H}}_{\mathrm{pd}} &\leq -\frac{\epsilon}{2} \begin{bmatrix} \|\tilde{\boldsymbol{q}}\| \\ \|\dot{\tilde{\boldsymbol{q}}}\| \end{bmatrix}^{\mathrm{T}} \boldsymbol{Q}_{\mathrm{nl}} \begin{bmatrix} \|\tilde{\boldsymbol{q}}\| \\ \|\dot{\tilde{\boldsymbol{q}}}\| \end{bmatrix} + \delta + \boldsymbol{\zeta}_u^{\mathrm{T}} \boldsymbol{z}'_u; \\ \boldsymbol{Q}_{\mathrm{nl}} &= \begin{bmatrix} 2\lambda_{\mathrm{m}}(\mathcal{K}_\beta) & -\lambda_{\mathrm{M}}(\mathcal{K}_v) \\ -\lambda_{\mathrm{M}}(\mathcal{K}_v) & \frac{1}{\epsilon}\lambda_{\mathrm{m}}(\mathcal{K}_v) \end{bmatrix}. \end{aligned} \tag{38}$$

with δ as in (25). Using the storage and Lyapunov functions $\mathcal{H}_{\mathrm{pd}}$ and $V_2 = \mathcal{H}_{\mathrm{pd}} + \mathcal{H}_{\mathrm{i}}$, with the definitions in (15) and (36), we can complete the proof following the steps in Prop. 1. □

VI. Delayed PID Control

From Proposition 1, it is evident that only *local* asymptotic stability is assured (analogous to the rigid robot case, c.f. [29]). The presence of the cross term $\epsilon k_c ||\tilde{\boldsymbol{q}}|| \, ||\dot{\tilde{\boldsymbol{q}}}||^2$ in (25) and (38) impedes us from claiming OSP and asymptotic stable setpoint control in the *global* sense. To deal with this problematic term, we can adopt *nonlinear* PID controllers [26], [27] and normalize the cross term by modifying ϵ to a non-constant term, as in [30]. However, motivated by the observation that it is customary to activate the integral term only when the output is "close" to its desired value to avoid overshooting, we adopted the delayed PID controller from Loria [18]. The idea is to patch together a globally and locally asymptotically stable controller, where the former drives the solution into an

[4]For simplicity, we neglect externals forces on the motor inertias.

[5]Note that equations (31), (32) and (33) correspond to (39), (A7) and (A10) in [21], with $\boldsymbol{A} = \boldsymbol{\kappa}^{-1}(\boldsymbol{\varphi})\boldsymbol{\kappa}(\bar{\boldsymbol{\varphi}})$ and $\boldsymbol{a} = (\boldsymbol{I} - \boldsymbol{A})\dot{\boldsymbol{q}}_u + \boldsymbol{\kappa}^{-1}(\boldsymbol{\varphi})\dot{\bar{\boldsymbol{u}}}_u$. A physical interpretation of the transformation (31) and a detailed derivation of (33) is provided in [21].

arbitrarily small domain of attraction of the latter one; see [31]. For the former, we choose the global ESP controller in [8].

Proposition 3 (ESP-PD control [8])**.** *Consider the transformed system* (5) *or* (33) *in closed loop with the PD feedback*

$$\bar{\boldsymbol{u}} = -\mathcal{K}_p\tilde{\boldsymbol{q}} - \mathcal{K}_v\dot{\tilde{\boldsymbol{q}}} + \frac{\partial \mathcal{V}_g}{\partial \bar{\boldsymbol{q}}}, \tag{39}$$

with the definitions in Remark 2. Then the closed loop is a passive map $\dot{\boldsymbol{q}}_u \mapsto \mathcal{Q}'_u$ *and, for* $\mathcal{Q}' = \mathbf{0}$*, globally asymptotically stable at the origin* $\boldsymbol{y} = (\tilde{\boldsymbol{q}}, \dot{\tilde{\boldsymbol{q}}}) = \mathbf{0}$*.*

Proof of Proposition 3. First, we notice that the closed loop (5) and (39) is a special case of the error dynamics (33) and (39); thus, this proof is concerned with the latter one. Using

$$V_3(\boldsymbol{y}) = \tfrac{1}{2}\big(\dot{\tilde{\boldsymbol{q}}}^{\mathrm{T}}\mathcal{M}\dot{\tilde{\boldsymbol{q}}} + \tilde{\boldsymbol{q}}^{\mathrm{T}}\mathcal{K}_p\tilde{\boldsymbol{q}}\big) + \mathcal{V}_e(\bar{\boldsymbol{\varphi}}), \tag{40}$$

as storage and Lyapunov candidate function, we get

$$\dot{V}_3 = -\dot{\tilde{\boldsymbol{q}}}^{\mathrm{T}}\mathcal{K}_v\dot{\tilde{\boldsymbol{q}}} + \dot{\tilde{\boldsymbol{q}}}_u^{\mathrm{T}}\mathcal{Q}'_u \tag{41}$$

and conclude the desired passivity property. Moreover, setting $\mathcal{Q}'_u = \mathbf{0}$, then global asymptotic stability of the origin $\boldsymbol{y} = \mathbf{0}$ immediately follows invoking Krasovskii–La'Salle's invariance principle [28]. □

Following [18], we can use Proposition 3 to formulate a globally asymptotically stable delayed PID controller.

Proposition 4 (Delayed ESP-PID Control)**.** *Consider, in absence of external force, i.e.,* $\mathcal{Q}' = \mathbf{0}$*, the transformed system* (5) *or* (33) *in closed loop with the PID feedback*

$$\bar{\boldsymbol{u}} = -\mathcal{K}_p\tilde{\boldsymbol{q}} - \mathcal{K}_v\dot{\tilde{\boldsymbol{q}}} + \frac{\partial \mathcal{V}_g}{\partial \bar{\boldsymbol{q}}} + \boldsymbol{v}, \tag{42}$$

$$\dot{\boldsymbol{v}}_u = \begin{cases} \mathbf{0}, & \boldsymbol{v}_u(0) = \mathbf{0} \in \mathbb{R}^n \quad \text{for } 0 \le t \le t_s \\ \boldsymbol{K}_i\tilde{\boldsymbol{q}}_u, & \boldsymbol{v}_u(t_s) = \mathbf{0} \in \mathbb{R}^{n/2} \text{ for } t \ge t_s \end{cases} \tag{43}$$

with the definitions in Remark 2. Then, there always exists a finite time constant $t_s \ge 0$*, a sufficiently large proportional gain* $\boldsymbol{K}_{pu}$ *and/or a sufficiently small integral gain* $\boldsymbol{K}_i$*, independent of the initial conditions, such that the closed-loop system is globally asymptotically stable at the origin* $\boldsymbol{x} = (\tilde{\boldsymbol{q}}, \dot{\boldsymbol{q}}, \boldsymbol{v}_u) = \mathbf{0}$*.*

Proof of Proposition 4. From Proposition 3, we know that during the first phase $\big(0 \le t \le t_s\big)$ of the delayed ESP-PID controller, $(\tilde{\boldsymbol{q}}(t), \dot{\boldsymbol{q}}(t)) \to \mathbf{0}$ as $t \to \infty$. Thus, for any strictly positive α, in the first phase the solution is driven into the domain of attraction B_α of the PID controllers in Proposition 1 and 2 in finite time. Next, let us lower bound V_2. By Taylor's Theorem [32], $\mathcal{V}_e(\bar{\boldsymbol{\varphi}}) = \frac{1}{2}\bar{\boldsymbol{\varphi}}^{\mathrm{T}}\frac{\partial^2 \mathcal{V}_e(r\bar{\boldsymbol{\varphi}})}{\partial \bar{\boldsymbol{\varphi}}^2}\bar{\boldsymbol{\varphi}}$ for some r, $1 \ge r \ge 0$, which implies that $\mathcal{V}_e(\bar{\boldsymbol{\varphi}}) \ge \frac{c_m}{2}\|\bar{\boldsymbol{\varphi}}\|^2$, and hence $V_2 \ge \frac{\lambda}{2}\{c_m\|\bar{\boldsymbol{\varphi}}\|^2 + \lambda_{\mathrm{m}}(\boldsymbol{K}_{pu})\|\tilde{\boldsymbol{q}}_u\|^2\} = \frac{\lambda}{2}\tilde{\boldsymbol{q}}^{\mathrm{T}}\mathcal{K}_m\tilde{\boldsymbol{q}}$, where

$$1 > \lambda > 0, \quad \mathcal{K}_m = \begin{bmatrix} \{\lambda_{\mathrm{m}}(\boldsymbol{K}_{pu}) + c_m\}\boldsymbol{I} & -c_m\boldsymbol{I} \\ -c_m\boldsymbol{I} & c_m\boldsymbol{I} \end{bmatrix}.$$

Continuing similarly to [18], let us derive an upper bound for α using $V_2^m = \frac{\lambda}{2}\lambda_{\mathrm{m}}(\mathcal{K}_m)\|\tilde{\boldsymbol{q}}\|^2$ and the set $B_\alpha^m = \{\boldsymbol{x} \in \mathbb{R}^{3n} \colon V_2^m(\boldsymbol{x}) \le \alpha\}$. It immediately follows from the definitions that $V_2^m \le V_2$ and $B_\alpha \subset B_\alpha^m$; thus, $\dot{V}_2(B_\alpha^m) \le 0$ implies that $\dot{V}_2(B_\alpha) \le 0$. We know that condition (19), i.e., $\|\tilde{\boldsymbol{q}}\| \le d$, with $d = [\lambda_{\mathrm{m}}(\mathcal{K}_v)/(2\epsilon) - \lambda_{\mathrm{M}}(\mathcal{M})]/k_c$, is sufficient to ensure that $\dot{V}_2(\boldsymbol{x}) \le 0$. Thus, for $\|\tilde{\boldsymbol{q}}\| \le d$ and $\dot{V}_2(B_\alpha^m) \le 0$ to hold true it should be that $\alpha \le \frac{1}{2}\lambda\lambda_{\mathrm{m}}(\mathcal{K}_m)d^2$. Finally, to ensure global asymptotic stability of the origin $\boldsymbol{x} = \mathbf{0}$, it is sufficient to choose the time t_s as the first time instant when $\boldsymbol{x}(t_s) \in B_\alpha$, that is,

$$t_s \colon V_2\big(\boldsymbol{x}(t_s)\big) \le \alpha. \qquad \square$$

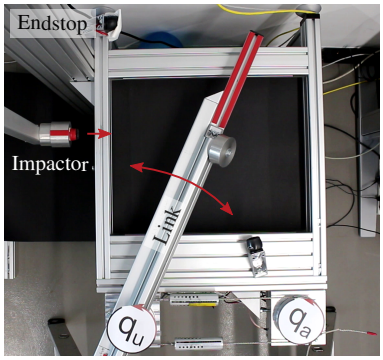

Figure 3. A series elastic actuator testbed with impactor.

Remark 3. *In practice, we can also employ a state-dependent switching, that is, activate the second case in* (43) *as soon as* $\tilde{\boldsymbol{q}}$ *satisfies* (19)*.*

Remark 4. *The link acceleration and jerk signals can be expressed in terms of the robot states* $(\boldsymbol{q}, \dot{\boldsymbol{q}})$ *using the model* (1)*; see appendix of [33] for details. Exploiting this property allows writing the final control law* $\boldsymbol{u}$*, constituted by* (4),(42)–(43)*, in the desired (dynamic state feedback) form* $\boldsymbol{u} = \boldsymbol{f}(\boldsymbol{q}, \dot{\boldsymbol{q}}, \boldsymbol{v}_u)$*.*

VII. Experimental Setup

This section introduces the experimental setups, the employed integrator logic and reports experimental validation of the proposed controller. We offer an experimental comparison with the state of the art controllers reported in [6], [13], see eq. (26), and [34]; referred to as C1, C2 and C3. C1 is a joint impedance controller developed for lightweight robots with inherent joint elasticity such as LWR III. C2 is a robust PID controller with non-collocated integral action; a critical feature shared by our controller (ESP-PID). ESP-PID and C2 share the same PID gain layout as in Table I, but with a damping ratio of 2 for C2. The gains for C1 were obtained by manual tuning; following the notation in [6]: $K_{qd} = k_{pu}$, $D_\theta = 52.9\,\mathrm{N\,m\,rad^{-1}\,s}$, $B_\theta = 0.65B$, $D = 1.72\,\mathrm{N\,m\,rad^{-1}\,s}$. C3 has the same structure as C1, but with integral feedback.

A. Hardware

We will study the performance of the proposed controllers on two different robots. The first is a dedicated SEA testbed, and the second, DLR *David*, is a soft robot. Table I summarizes critical system and control parameters. We employed a fourth-order derivative filter with a cut-off frequency of 80 Hz for either system to obtain velocity signals. We used the momentum observer [5] to compensate motor friction and estimate $\mathcal{Q}'_u$.

The SEA testbed is constituted by an LWR III motor unit and elastic elements from DLR C-Runner, and moves in the horizontal plane, as depicted in Fig. 3. See [33] for details. This

Table I
SYSTEM AND CONTROL PARAMETERS

	David	Testbed
Link inertia	n.a.	$1\,\mathrm{kg\,m^2}$
Motor inertia	$0.3117\,\mathrm{kg\,m^2}$	$0.6\,\mathrm{kg\,m^2}$
Joint stiffness	52.4–826 $\mathrm{N\,m\,rad^{-1}}$	$362\,\mathrm{N\,m\,rad^{-1}}$
Actuator limits	$\pm 67\,\mathrm{N\,m}$	$\pm 100\,\mathrm{N\,m}$
Link sensor resolution	16 bit / 271°	23 bit / revolution
Controller rate	3000 Hz	3000 Hz
P gain [$\mathrm{N\,m\,rad^{-1}}$]	$\boldsymbol{K}_{pu,ii} = 100$	$k_{pu} = 200$
I gain [$\mathrm{N\,m\,rad^{-1}\,s^{-1}}$]	$\boldsymbol{K}_{i,ii} = 1000$	$k_i = 200$
D gain [$\mathrm{N\,m\,rad^{-1}\,s}$]	$\xi_u = 0.6, \xi_a = 0.1$	$\xi_u = 0.7, \xi_a = 0.3$
Inertia shaping	reduced to $0.3\boldsymbol{B}$	no

basic setup is intended to demonstrate the achievable control performance in a scenario where the dynamics of the actual hardware matches the considered model (1) closely.

DLR *David* [15], as shown in Fig. 1, is implemented with variable stiffness actuators. For the experiments, we considered the first four main axes. The applied stiffness setting corresponds to the stiffness profile shown in blue in Fig. 1. We followed the damping design reported in [16] and ξ_u and ξ_a refer to the link- and motor-side modal damping factors.

B. Integrator Logic

Practical experience suggests activating integral action only when $\tilde{\boldsymbol{q}}_u$ is close to zero to reduce overshooting, and deactivating it when $\tilde{\boldsymbol{q}}_u$ becomes large to avoid undesirable transient behavior. A common difficulty in using integral action is the presence of stick-slip effects, which can cause oscillations due to the interplay of integral gains and friction nonlinearities [20]. To alleviate this issue, deactivating the integral action is customary when $\tilde{\boldsymbol{q}}_u$ is very small. It is worth mentioning that we did not encounter such oscillations with the reported integral gains on *David* or the SEA testbed. The integrator logic in Algorithm 1 applies to each joint individually and evolves around two critical events: 1) the estimated external torque $\hat{\mathcal{Q}}'_{ui}$ surpasses some threshold δ_c, with $\delta_c = 1\,\mathrm{N\,m}$ for the SEA and $\delta_c = 6\,\mathrm{N\,m}$ for *David*, 2) the position error grows too large, i.e., $\tilde{q}_{ui} \geq \delta_q$ with $\delta_q = 2°$ for both systems. For each system, the noise level of the corresponding momentum observer dictates a lower bound on δ_c. Remark 3 provides justification for a position-error-based switching event; theoretically, δ_q should be linked to (19). For practical purposes, however, δ_q should be treated as a joint-specific tuning parameter. Clamping is used to avoid integrator windup. Regarding Algorithm 1, line 6 corresponds to the global PD controller in Proposition 3 and line 8 to the local PID controller in Proposition 1 and 2. The case $\mathcal{Q}_u \neq \mathbf{0}$ in line 4 does not allow for a "standard" stability analysis, but the passivity conclusions of Proposition 1 and 2 hold. In this case, $\boldsymbol{v}_u$ is constant and thus can be treated as a constant external force on the unactuated subsystem of $\bar{\Sigma}_{pd}$.

Algorithm 1: Integrator logic applies to each joint individually

Inputs: $\tilde{q}_{ui}, \dot{q}_{ui}, \hat{\mathcal{Q}}'_{ui}$
Outputs: $v_{ui}, \dot{v}_{ui}, \ddot{v}_{ui}$
1: INIT: $v_{ui} = 0$, $\dot{v}_{ui} = 0$, $\ddot{v}_{ui} = 0$
2: **while** System running **do**
3: **if** $|\hat{\mathcal{Q}}'_{ui}| > \delta_c$ **then**
4: HOLD: v_{ui} holds present value, $\dot{v}_{ui} = 0$, $\ddot{v}_{ui} = 0$
5: **else if** $|\tilde{q}_{ui}| > \delta_q$ **then**
6: OFF: v_{ui}, $\dot{v}_{ui} = 0$, $\ddot{v}_{ui} = 0$
7: **else**
8: ON: integrator initializes with the last value of v_{ui}
$v_{ui} = \int_0^t k_i \tilde{q}_{ui}(\tau) d\tau$, $\dot{v}_{ui} = k_i \tilde{q}_{ui}$, $\ddot{v}_{ui} = k_i \dot{\tilde{q}}_{ui}$
9: **end if**
10: **end while**

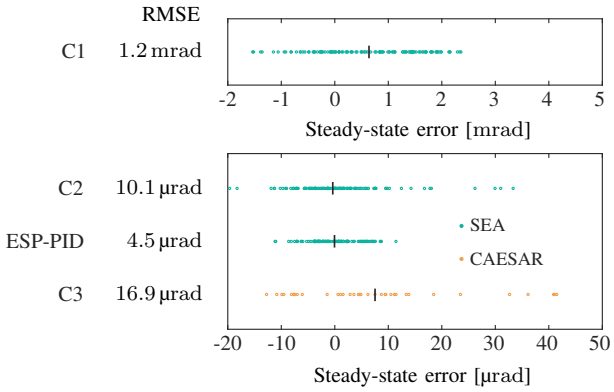

Figure 4. Link-side positioning accuracy: elastic versus rigid joint. The arithmetic means (black bars) and root-mean-square errors (RMSE) are shown.

VIII. EXPERIMENTAL RESULTS

a) Testbed: Elastic vs. Rigid Actuators: Figure 4 best summarizes the overall conclusion drawn from the following experiments, which presents the positioning accuracy achieved by: 1) C3 on a testbed constituted by a single "rigid" actuator of the space robot CAESAR [34], 2) C1, C2 and ESP-PID on a dedicated SEA testbed. In total, ten different reference link positions were selected, and each approached from both directions from three different distances. This procedure was executed twice for a total number of 120 data points. The distances were selected to exhibit both "slow" friction-dominated behavior (static and Stribek friction) and "fast" inertial force-dominated behavior. In summary, the integrator-based schemes (bottom) reduce the steady-state errors by two orders of magnitudes compared to C2. ESP-PID approaches the link sensor resolution of $0.75\,\mu\mathrm{rad}$, while C3 is limited in its accuracy by the link sensor resolution of $16.9\,\mu\mathrm{rad}$.

b) Testbed: Step Response and Disturbance Rejection: Figure 5 shows exemplary the disturbance rejection and set-point control performance of the compared controllers. Note that ESP-PID achieves a satisfactory disturbance rejection behavior despite input saturation during a collision with the impactor, as shown in Fig. 3. Comparing the performance of the different controllers, we conclude that 1) non-collocated integral action successfully reduces the steady state error, 2) "direct" damping through non-collocated velocity feedback improves the transient and disturbance rejection behavior, 3) the robustness of a control design does not necessarily suffer from relying on link and acceleration signals. Latter observation can possibly be explained by the technique noted in Remark 4.

c) David: Set-point and Motion Tracking Control: In practice, the tracking problem is often solved by regulating the link positions about a time-varying trajectory. Figure 6 shows the performance of the ESP-PID on *David*. As expected from a regulation controller, the tracking error approaches zero only in

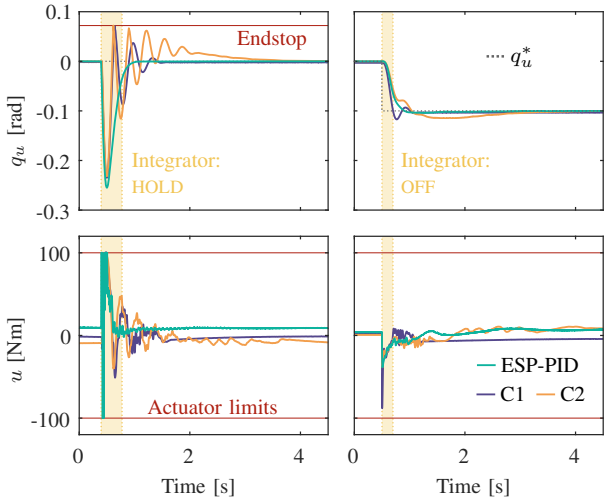

Figure 5. (**Left**): the impactor exerts a peak force of approximately $\hat{\mathcal{Q}}'_u = 330\,\mathrm{N\,m}$ at around $t = 0.5\,\mathrm{s}$. (**Right**): A step is commanded.

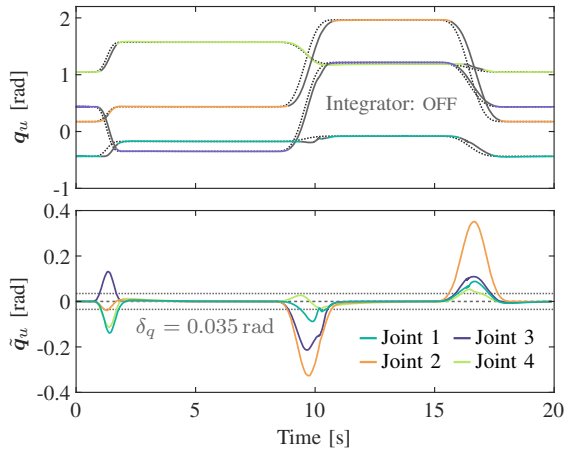

Figure 6. Delayed PID controller on *David*.

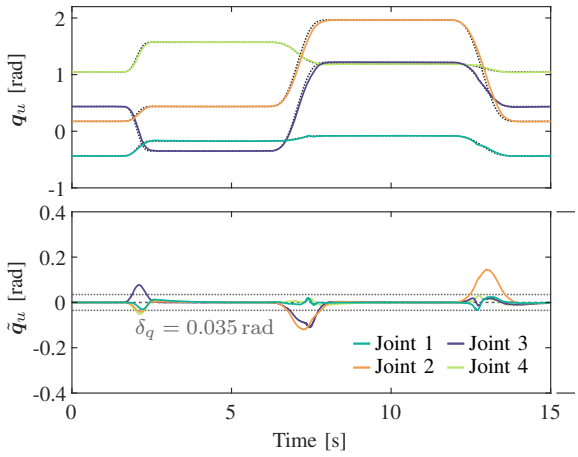

Figure 7. Delayed PID controller "patched" with a motion tracking controller [16] on *David*.

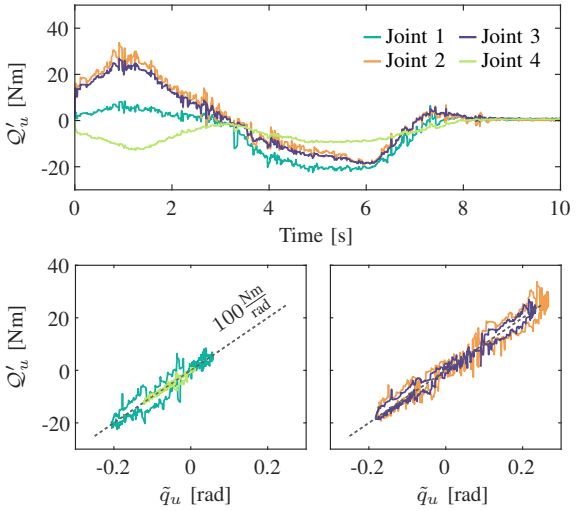

Figure 8. (**Top**) Time variations of the external torques. (**Bottom**) External torque versus joint deflections for the first four joints.

phases where the desired velocity is zero. Gravity compensation combined with a state-dependent damping design may enable overshoot-free transients [16]. By replacing the regulation controller with a globally asymptotically stable tracking controller in phases where integral terms are deactivated, we can expect to improve the transient performance. Figure 7 considers such case by combining the tracking controller from [16] with the proposed delayed PID controller; resulting in an improved transient performance. However, the presented stability results would require some extension to cover such a case.

d) David: Disturbance Rejection & Impedance Behavior: A human user applies forces on the end-effector by pushing and pulling on the robot's hand. The exerted torques are reported in Fig. 8 (top), and Fig. 8 (bottom) reports the associated torque-deflection relations. We can observe that the results closely approximate the desired steady-state behavior (dashed line). Figure 9 shows the disturbance rejection performance due to external forces imposed by a human. For comparison, using a stiff motor controller reveals the intrinsic oscillatory dynamics of the system, as shown in Figure 9 (bottom). We conclude that the desired compliance in contact is not impaired thanks to the integrator logic. Furthermore, the robustness towards disturbances is demonstrated, see also the attached video.

IX. Conclusions

This work addressed the practically relevant problem of compensating steady-state errors in the setpoint control of elastic joint robots. Following the structure preserving design philosophy of ESP control, we achieved a link-side PID control structure with delayed integral action, ensuring global asymptotic stability in free motion and passivity during an interaction. By preserving desired physical properties such as passivity—and refraining from canceling manipulator nonlinearities or the motor dynamics—the design is expected to be robust. The impact and interaction experiments support this hypothesis. The experiments further demonstrate that the proposed controller combines excellent positioning accuracy with compliant interaction in contact. Steady-state errors caused by, e.g., friction or uncertain gravity knowledge, are successfully compensated, and the final errors are close to the sensor resolution. Good transients without overshooting are achieved throughout the workspace by combining non-collocated PID action with gravity compensation and by activating the integral action only close to the desired position.

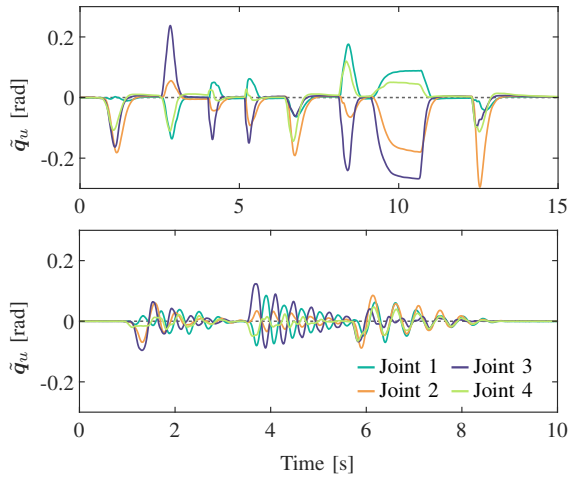

Figure 9. (**Top**) Disturbance rejection behavior of the delayed PID controller. (**Bottom**) Disturbance rejection of a "stiff" PD controller with motor position and velocity feedback highlighting *David's* intrinsic oscillatory dynamics.

Compliant and rigid robots may each have their advantages and disadvantages. However, when it comes to positioning accuracy, they are potentially on equal footing, as highlighted in this work. Future research is needed to achieve a similar level of accuracy in motion tracking.

X. Appendix

We can rewrite the storage function (16) as

$$\mathcal{H}_{\text{PD}} = \tfrac{1}{2}\Big[\boldsymbol{\zeta}^{\mathrm{T}}\mathcal{M}\boldsymbol{\zeta} + \tilde{\boldsymbol{q}}^{\mathrm{T}}(\mathcal{K}' - \epsilon^2\mathcal{M})\tilde{\boldsymbol{q}}\Big],$$

which is positive definite in $(\tilde{\boldsymbol{q}}, \dot{\tilde{\boldsymbol{q}}})$ since ϵ satisfies (17).

References

[1] G. Hirzinger, N. Sporer, A. Albu-Schäffer, M. Hahnle, R. Krenn, A. Pascucci, and M. Schedl, "Dlr's torque-controlled light weight robot iii-are we reaching the technological limits now?" *2002 IEEE Int. Conf. on Robotics and Automation*, vol. 2, pp. 1710–1716, 5 2002.

[2] R. Alami, A. Albu-Schäffer, A. Bicchi, R. Bischoff, R. Chatila, A. De Luca, A. De Santis, G. Giralt, J. Guiochet, G. Hirzinger, F. Ingrand, V. Lippiello, R. Mattone, D. Powell, S. Sen, B. Siciliano, G. Tonietti, and L. Villani, "Safe and dependable physical human-robot interaction in anthropic domains: State of the art and challenges," *2006 IEEE/RSJ Int. Conf. on Intelligent Robots and Systems*, pp. 1–16, 2006.

[3] G. Tonietti, R. Schiavi, and A. Bicchi, "Design and control of a variable stiffness actuator for safe and fast physical human/robot interaction," in *IEEE Int. Conf. on Robotics and Automation*, 4 2005, pp. 526–531.

[4] B. Vanderborght, A. Albu-Schäffer, A. Bicchi, E. Burdet, D. G. Caldwell, R. Carloni, M. Catalano, O. Eiberger, W. Friedl, G. Ganesh, *et al.*, "Variable impedance actuators: A review," *Robotics and Autonomous Syst.*, vol. 61, no. 12, pp. 1601–1614, 2013.

[5] A. De Luca, A. Albu-Schäffer, S. Haddadin, and G. Hirzinger, "Collision detection and safe reaction with the dlr-iii lightweight manipulator arm," *2006 IEEE/RSJ IROS*, pp. 1623–1630, 2006.

[6] A. Albu-Schäffer, C. Ott, and G. Hirzinger, "A unified passivity-based control framework for position, torque and impedance control of flexible joint robots," *The Int. J. of Robotics Research*, vol. 26, no. 1, pp. 23–39, 2007.

[7] R. Schiavi, G. Grioli, S. Sen, and A. Bicchi, "Vsa-ii: A novel prototype of variable stiffness actuator for safe and performing robots interacting with humans," in *2008 IEEE Int. Conf. on Robotics and Automation*. IEEE, 2008, pp. 2171–2176.

[8] M. Keppler, D. Lakatos, C. Ott, and A. Albu-Schäffer, "Elastic structure preserving impedance (ESπ)control for compliantly actuated robots," *IEEE/RSJ Int. Conf. on Intelligent Robots & Sys.*, pp. 5861–5868, 2018.

[9] Y. Lin, Z. Chen, and B. Yao, "Decoupled torque control of series elastic actuator with adaptive robust compensation of time-varying load-side dynamics," *IEEE Transactions on Industrial Electronics*, vol. 67, no. 7, pp. 5604–5614, 2020.

[10] L. Le-Tien and A. O. Albu-Schäffer, "Robust adaptive tracking control based on state feedback controller with integrator terms for elastic joint robots with uncertain parameters," *IEEE Transactions on Control Systems Technology*, vol. 26, pp. 2259–2267, 2018.

[11] A. Izadbakhsh and P. Kheirkhahan, "Nonlinear pid control of electrical flexible joint robots-theory and experimental verification," *IEEE Int. Conf. on Industrial Technology*, pp. 250–255, 2018.

[12] Y. Wang, H. Yu, J. Yu, H. Wu, and X. Liu, "Trajectory tracking of flexible-joint robots actuated by pmsm via a novel smooth switching control strategy," *Applied Sciences*, vol. 9, no. 20, p. 4382, 2019.

[13] A. A. Pervozvanski and L. B. Freidovich, "Robust stabilization of robotic manipulators by pid controllers," *Dynamics and Control*, vol. 9, pp. 203–222, 1999.

[14] Q. Zhang and G. Liu, "Precise control of elastic joint robot using an interconnection and damping assignment passivity-based approach," *IEEE/ASME Trans. on Mechatronics*, vol. 21, pp. 2728–2736, 2016.

[15] M. Grebenstein, A. Albu-Schäffer, T. Bahls, M. Chalon, O. Eiberger, W. Friedl, R. Gruber, S. Haddadin, U. Hagn, R. Haslinger, H. Höppner, S. Jörg, M. Nickl, A. Nothhelfer, F. Petit, J. Reill, N. Seitz, T. Wimböck, S. Wolf, T. Wüsthoff, and G. Hirzinger, "The dlr hand arm system," in *IEEE Int. Conf. on Robotics and Automation*, 2011, pp. 3175–3182.

[16] M. Keppler, D. Lakatos, C. Ott, and A. Albu-Schäffer, "Elastic structure preserving (ESP) control for compliantly actuated robots," *IEEE Transactions on Robotics*, vol. 34, no. 2, pp. 317–335, 2018.

[17] A. Albu-Schäffer, O. Eiberger, M. Grebenstein, S. Haddadin, C. Ott, T. Wimbock, S. Wolf, and G. Hirzinger, "Soft robotics," *IEEE Robotics Automation Magazine*, vol. 15, no. 3, pp. 20–30, 9 2008.

[18] A. Loria, A. Lefeber, and H. Nijmeijer, "Global asymptotic stability of robot manipulators with linear pid and pi2d control," *Stability and Control: Theory and Applications*, vol. 3, no. 2, pp. 138–149, 2000.

[19] A. Bisoffi, M. Da Lio, A. R. Teel, and L. Zaccarian, "Global asymptotic stability of a pid control syst. with coulomb friction," *IEEE Transactions on Automatic Control*, vol. 63, no. 8, pp. 2654–2661, 2017.

[20] C. C. de Wit, B. Siciliano, and G. Bastin, *Theory of robot control*. Springer Science & Business Media, 2012.

[21] M. Keppler, C. Ott, and A. Albu-Schäffer, "From underactuation to quasi-full actuation: Aiming at a unifying control framework for articulated soft robots," *Int. J. of Robust and Nonlinear Control*, 2022.

[22] A. De Luca and F. Flacco, "Dynamic gravity cancellation in robots with flexible transmissions," in *IEEE Conf. on Decision and Control*, 2010, pp. 288–295.

[23] M. W. Spong, "Modeling and control of elastic joint robots," *J. of Dynamic Sys., Measurement, and Control*, vol. 109, pp. 310–319, 1987.

[24] R. Kelly, V. S. Davila, and J. A. L. Perez, *Control of Robot Manipulators in Joint Space*. Springer Science & Business Media, 2006.

[25] D. Koditschek, "Natural motion for robot arms," *IEEE Conf. on Decision and Control*, 1984.

[26] R. Ortega, *Passivity-based Control of Euler-Lagrange Systems: Mechanical, Electrical, and Electromechanical Applications*. Springer, 1998.

[27] S. Arimoto, "A class of quasi-natural potentials and hyper-stable pid servo-loops for nonlinear robotic systems," *Journal of the Society of Instrument and Control Engineers*, vol. 30, pp. 1005–1012, 1994.

[28] H. K. Khalil, *Nonlinear Systems*, 3rd ed. Prentice Hall, 2001.

[29] J. T. Wen and S. H. Murphy, "PID control for robot manipulators," *Rensselaer Polytechnic Institute Troy, NY, USA*, 1990.

[30] L. L. Whitcomb, A. A. Rizzi, and D. E. Koditschek, "Comparative experiments with a new adaptive controller for robot arms," *IEEE Trans. on Robotics and Automation*, vol. 9, no. 1, pp. 59–70, 1993.

[31] A. R. Teel and N. Kapoor, "Uniting local and global controllers," in *1997 European Control Conference (ECC)*. IEEE, 1997, pp. 3868–3873.

[32] K. Königsberger, *Analysis 2*. Springer-Verlag, 2013.

[33] M. Keppler, F. Loeffl, D. Wandinger, C. Raschel, and C. Ott, "Analyzing the performance limits of articulated soft robots based on the ESPi framework: Applications to damping and impedance control," *IEEE Robotics and Automation Letters*, vol. 6, no. 4, pp. 7121–7128, 2021.

[34] A. Beyer, G. Grunwald, M. Heumos, M. Schedl, R. Bayer, W. Bertleff, B. Brunner, R. Burger, J. Butterfass, R. Gruber, *et al.*, "Caesar: Space robotics technology for assembly, maintenance, and repair," *Proceedings of the International Astronautical Congress, IAC*, 2018.